



## RESEARCH ARTICLE

10.1029/2024JG008226

Terrestrial Organic Matter Contributes to CO<sub>2</sub> Production From Siberian Shelf SedimentsLewis Sauerland<sup>1,2</sup> , Nicholas Ray<sup>1,3</sup> , Jannik Martens<sup>1,2,4</sup> , Tommaso Tesi<sup>5</sup> , Oleg Dudarev<sup>6,7,8</sup>, Örjan Gustafsson<sup>1,2</sup> , Igor Semiletov<sup>6,7,8</sup>, and Birgit Wild<sup>1,2</sup> 

## Key Points:

- Carbon dioxide fluxes from sediment slurry incubations showed high variability and were dependent on the input of terrestrial organic matter
- Pronounced variability in oxygen consumption of intact sediment cores could not be explained by the input of terrestrial organic matter

## Supporting Information:

Supporting Information may be found in the online version of this article.

## Correspondence to:

L. Sauerland and B. Wild,  
[Lewis.Sauerland@aces.su.se](mailto:Lewis.Sauerland@aces.su.se);  
[birgit.wild@aces.su.se](mailto:birgit.wild@aces.su.se)

## Citation:

Sauerland, L., Ray, N., Martens, J., Tesi, T., Dudarev, O., Gustafsson, Ö., et al. (2025). Terrestrial organic matter contributes to CO<sub>2</sub> production from Siberian shelf sediments. *Journal of Geophysical Research: Biogeosciences*, 130, e2024JG008226. <https://doi.org/10.1029/2024JG008226>

Received 21 MAY 2024

Accepted 25 NOV 2024

<sup>1</sup>Department of Environmental Science, Stockholm University, Stockholm, Sweden, <sup>2</sup>Bolin Centre for Climate Research, Stockholm University, Stockholm, Sweden, <sup>3</sup>School of Marine Science and Policy, University of Delaware, Lewes, DE, USA, <sup>4</sup>Lamont-Doherty Earth Observatory of Columbia University, New York, NY, USA, <sup>5</sup>Institute of Polar Sciences, National Research Council, Bologna, Italy, <sup>6</sup>Il'ichov Pacific Oceanological Institute (POI), Far-East Branch of the Russian Academy of Sciences, Vladivostok, Russia, <sup>7</sup>International Centre of the Far-Eastern and Arctic Seas Named By Admiral S. O. Makarov, Sakhalin 17 State University-SakhalinTECH (SakhGU), Yuzhno-Sakhalinsk, Russia, <sup>8</sup>Tomsk State University (TSU), Tomsk, Russia

**Abstract** Arctic climate warming is causing permafrost thaw and erosion, which may lead to enhanced inputs of terrestrial organic matter into Arctic Ocean shelf sediments. Degradation of terrestrial organic matter in sediments might contribute to carbon dioxide production and bottom water acidification. Yet, the degradability of organic matter in shallow Arctic Ocean sediments, as well as the contribution of terrestrial input, is poorly quantified. Here, potential organic matter degradation rates were investigated for 16 surface sediments from the Kara Sea, Laptev Sea, and the western East Siberian Sea and compared with physicochemical sediment properties including molecular biomarkers, stable and radioactive carbon isotopes, and grain size. Aerobic oxygen and carbon dioxide fluxes, measured in laboratory incubations of sediment slurry, showed high spatial variability and correlated significantly with organic carbon content as well as with the amount and degradation state of terrestrial organic matter. The dependency on terrestrial organic matter declined with increasing distance from land, indicating that the presence of terrestrial organic matter is likely a constraining factor for organic matter degradation in shallow shelf seas. However, sediment oxygen consumption rates, measured in incubations of intact sediment cores, also exhibited substantial spatial variability but were not related to organic carbon content or terrestrial influence. Oxygen consumption of intact sediments may be more strongly influenced by in situ redox conditions. Together with previous observations, our findings support that terrestrial organic matter is easily degradable in shelf sea sediments and might substantially contribute to aerobic carbon dioxide production and oxygen consumption.

**Plain Language Summary** The Arctic climate is warming rapidly, which is leading to thawing of frozen deposits on land. These deposits contain large amounts of terrestrial organic matter that is being eroded and deposited into shallow ocean sediments. The breakdown of terrestrial organic matter in sediments might contribute to carbon dioxide release into the ocean water. There is insufficient knowledge on how fast this breakdown is happening and which parameters influence it. We investigated organic matter breakdown rates for sediment samples taken from shallow Siberian seas and compared them with sediment properties. Oxygen consumption and carbon dioxide release were measured in laboratory experiments and showed high variability between different samples. The release was related to the amount of terrestrial organic matter and its state of decomposition. This relationship decreased strongly for sediments further away from land. During a second incubation experiment, using intact sediment cores, oxygen consumption rates were measured and also showed high variability between samples. Oxygen consumption rates were not related to organic matter content. These findings support previous observations that terrestrial organic matter breaks down rapidly in shallow Arctic Ocean sediments and might also substantially contribute to the release of carbon dioxide and consumption of oxygen from the seawater.

## 1. Introduction

The Arctic is warming more rapidly than the global average due to polar amplification (Rantanen et al., 2022; You et al., 2021). The combined effects of higher air and ground temperatures, as well as sea ice retreat, lead to increasing rates of coastal erosion along the permafrost-dominated shorelines of the Arctic shelf seas (Jones

© 2025. The Author(s).

This is an open access article under the terms of the [Creative Commons Attribution License](https://creativecommons.org/licenses/by/4.0/), which permits use, distribution and reproduction in any medium, provided the original work is properly cited.

et al., 2020; Nielsen et al., 2022). Increased river discharge combined with destabilization and mobilization of permafrost soils and deposits in river catchments may lead to increasing inputs of terrestrial organic matter (terrOM) into fluvial systems, and eventually the Arctic Ocean (Feng et al., 2021; Hugelius et al., 2020; Peterson et al., 2002; Savelieva et al., 2000; Vonk & Gustafsson, 2013).

The Siberian shelf seas represent an area of the Arctic Ocean that receives substantial amounts of terrOM mobilized by coastal erosion and discharge of major rivers such as the Ob, Yenisey, Lena, and Kolyma rivers (Jakobsson et al., 2003; Martens et al., 2022; Stein and Macdonald, 2013). Terrestrially derived organic matter entering Arctic shelf seas contributes to sediment organic matter content, often exceeding 50% on the Siberian shelves (Gustafsson et al., 2011; Martens et al., 2022; Semiletov et al., 2011; Vonk et al., 2010, 2012). Terrestrial biomarker contents such as lignin phenols and high molecular weight (HMW) *n*-alkanes decrease by one to two orders of magnitude from nearshore to the outer shelf sediments (Matsubara et al., 2022). Additionally, lignin phenol and *n*-alkane degradation proxies (e.g., acid/aldehyde ratios of lignin and carbon preference index of HMW *n*-alkanes) indicate higher decomposition state of terrOM further from shore with proxy values changing by ca. one order of magnitude (Matsubara et al., 2022; Tesi et al., 2014). This shows that terrOM represents a labile pool of organic matter in shelf sediments that is readily decomposed to carbon dioxide (CO<sub>2</sub>).

The rates of organic matter decomposition in the water column, and sediments are important parameters that have cascading effects within the Arctic. Organic matter degradation releases CO<sub>2</sub>, which may be emitted to the atmosphere. The release of CO<sub>2</sub> also affects the Arctic Ocean carbonate system by lowering the pH of seawater, leading to acidification (Semiletov, 1999) that threatens carbonate shell-forming organisms and the food webs that depend on them (Capelle et al., 2020). Strong ocean acidification was observed on the Siberian Arctic Ocean shelves exceeding the levels expected by ocean uptake of rising atmospheric CO<sub>2</sub> alone, and attributed to the release of CO<sub>2</sub> from terrOM degradation (Semiletov et al., 2016). Thus, an increase in terrOM input caused by Arctic warming and permafrost thaw could affect organic matter degradation rates and have further reaching effects on the biogeochemistry of the Arctic marine environment.

Sediment oxygen (O<sub>2</sub>) consumption is frequently being used to estimate organic matter degradation rates in ocean sediments. In turn, sediment oxygen consumption can be utilized to estimate rates of sediment CO<sub>2</sub> production, using respiratory quotients (CO<sub>2</sub> flux/O<sub>2</sub> flux). However, such an approach is currently challenging in the Arctic Ocean for several reasons. First, despite a substantial number of O<sub>2</sub> consumption rates published for the Arctic Ocean, the Siberian shelf seas are notably under-represented (Bourgeois et al., 2017). Second, when sediment O<sub>2</sub> fluxes from the Laptev Sea, Kara Sea, and East Siberian Sea (ESS) are reported, they demonstrate high variability in space and disagreement between studies regarding relationships between sediment O<sub>2</sub> fluxes and depth and distance from shore (Boetius & Damm, 1998; Brüchert et al., 2018; Clough et al., 2005; Ray et al., 2024; Wollenburg & Kuhnt, 2000). Some of this variability could be associated with spatial and temporal differences in terrOM content and relative degradation state at the time of sampling. And third, sediment respiratory quotients in the world's oceans range from 0.69 to 1.31 (Jørgensen et al., 2022), making the association of O<sub>2</sub> consumption and CO<sub>2</sub> production difficult. Linking sediment terrOM content and degradation state with sediment O<sub>2</sub> consumption and respiratory quotients will help reduce uncertainty in understanding sediment O<sub>2</sub> consumption in Arctic shelf seas and allow for better estimates of sediment CO<sub>2</sub> production.

In this study, we investigated the decomposition potential of organic matter in sediments of the Kara Sea, Laptev Sea, and western ESS to deduce the influence of chemical and physical sediment properties, and in particular of terrOM. Therefore, potential CO<sub>2</sub> production and O<sub>2</sub> consumption rates were determined by incubating surface sediment samples as an aerobic slurry under controlled laboratory conditions. To assess which factors may affect CO<sub>2</sub> and O<sub>2</sub> fluxes, sediment samples were analyzed for elemental and isotopic composition (total organic carbon content (TOC), total nitrogen content (TN), δ<sup>13</sup>C-TOC, and Δ<sup>14</sup>C-TOC), grain size distribution, and molecular biomarkers reflecting the content, sources, and decomposition state of terrOM (lignin phenols and *n*-alkanes). Data from the laboratory incubation are compared with sediment O<sub>2</sub> consumption rates that were measured via shipboard incubations of intact sediment cores during the International Siberian Shelf Study expedition in fall 2020; these data were published previously in the context of sediment nitrous oxide dynamics and silicate cycling (Ray et al., 2024; Wild et al., 2023). We hypothesize that (a) high sediment TOC in general, and content of terrOM in particular, increases O<sub>2</sub> consumption and CO<sub>2</sub> production rates from Arctic shelf sediments, in both incubations of aerobic slurries and intact cores; (b) the effect of terrOM on O<sub>2</sub> and CO<sub>2</sub> fluxes is strongest close to land and diminishes further outward; and (c) correlations with the measured sediment characteristics will be weaker for

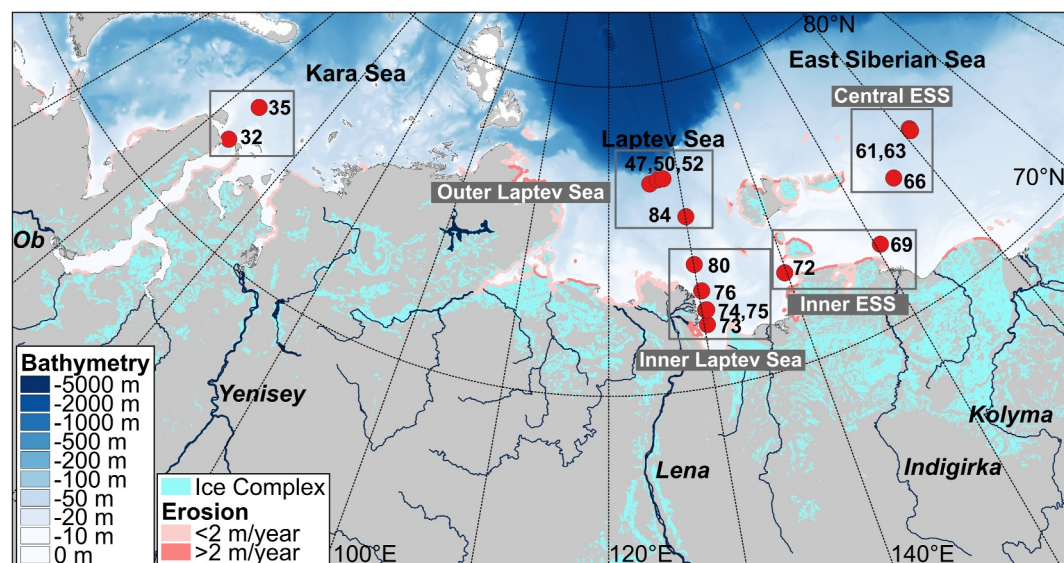


**Figure 1.** Map of the study area. All stations sampled for this study are marked with red dots. The map area shows the Siberian interior shelves including the Kara Sea, Laptev Sea, and East Siberian Sea (ESS). Stations within the Laptev Sea and ESS were clustered in four spatial subgroups that are marked with gray rectangles including outer Laptev Sea, inner Laptev Sea, inner ESS, and central ESS. Bathymetric data of IBCAO version 4 (Jakobsson et al., 2020), the extent of Ice Complex deposits (Strauss et al., 2021), and coastal erosion rates (Lantuit et al., 2012) are shown.

shipboard  $O_2$  fluxes of intact cores than for  $O_2$  and  $CO_2$  measured in laboratory slurry experiments as environmental factors are more variable during intact sediment core incubations.

## 2. Materials and Methods

### 2.1. Study Area

The area investigated in this study comprises the Kara, Laptev, and western ESS (Figure 1). These shallow interior shelf seas cover ca. 25% of the Arctic Ocean margin and extend up to 800 km seaward from land (Stein and Macdonald, 2013). The Kara Sea constitutes the western margin of the study area. Large seasonal freshwater discharge of the Ob and Yenisei river estuaries lead to pronounced stratification and large dissolved and suspended loads into the southern Kara Sea (Holmes et al., 2002; Osadchiev, Frey, Shchuka, et al., 2021). East of the Kara Sea, the Laptev Sea is separated from the ESS by the New Siberian Islands and the Dmitry Laptev Strait. Several rivers drain into the Laptev Sea with the Lena contributing >70% of the total discharge (Williams & Carmack, 2015). Parts of the coastline consisting of ice-rich permafrost deposits are influenced by strong coastal erosion (Fuchs et al., 2020; Holmes et al., 2002; Lantuit et al., 2012). The ESS constitutes the eastern margin of the study area. Its western part (until ca. 160°E) that is included in this study is dominated by river outflow of the Indigirka River and the eastward flow of fresher surface water from the Laptev Sea (Gordeev, 2000). Coastal erosion of destabilized ice-rich permafrost deposits contributes to inputs of terrOM into the western ESS (Semiletov et al., 2005).

### 2.2. Sediment Sampling

Sediment samples were collected during the International Siberian Shelf Study expedition in fall 2020 (ISSS-2020) on board the Russian *R/V Akademik Mstislav Keldysh*. Cores from 16 stations were used for this study, in most cases following transects from the mouths of large rivers (Ob, Lena, and Indigirka) toward the outer shelf, as shown in Figure 1. Sampling stations of the Laptev Sea and ESS were grouped according to their proximity to the Lena Delta or erosional coastlines, respectively. This distinction was further supported with water depth and bottom water salinity (Table S1 in Supporting Information S1). For the Laptev Sea, two groups were defined: the *inner Laptev Sea* consisting of stations close to the Lena Delta and the *outer Laptev Sea* with stations closer to the shelf break. Two stations located close to erosional coastlines along the ESS and Dmitry Laptev Strait were grouped as *inner ESS* (see Figure 1). Stations within the ESS that are situated further away from the coast were

grouped as *central ESS*. Sediment cores were collected using an Oktopus multicorer (ca. 10 cm core liner diameter). One core per station was used for shipboard incubations to determine sediment O<sub>2</sub> consumption and for the laboratory slurry incubation as described below. A second core was obtained for bulk sediment analysis (e.g., grain size, elemental composition, and biomarker). To this end, the core was sliced into 1-cm increments on board, and stored, transported, and continuously frozen until further usage. Freeze-dried material from 0–1 cm depth was used for the analyses described below. Stations sampled during the ISSS-2020 were numbered consecutively as AMK82-69XX, and station names are abbreviated here as the last two digits of the full name (e.g., 32 for AMK82-6932).

### 2.3. Shipboard Incubations

The processing of sediment cores and the setup of the shipboard sediment core incubation experiment, as well as O<sub>2</sub> measurements and calculations, are described in detail in Wild et al. (2023). Incubations lasted 10–14 days (see Table S7 in Supporting Information S1); the last stations sampled had shorter incubation times than the others to finish sample processing before the end of the expedition. Oxygen consumption rates from shipboard incubations are given as absolute values, that is, positive fluxes represent net sediment uptake. After the incubation, cores were sliced in 1-cm increments and stored frozen. The top 0–1 cm was used for laboratory slurry incubations.

### 2.4. Laboratory Slurry Incubations

Sediment slurry incubations were conducted under controlled laboratory conditions to determine simultaneous potential CO<sub>2</sub> production and O<sub>2</sub> consumption rates. Surface sediment samples (0–1 cm) from the shipboard incubation cores were thawed at 5°C and 10 g (wet) weighed into 125-mL glass incubation vessels. Triplicate incubations were created for each station sample. Artificial seawater was created by dissolving Instant Ocean sea salt mixture (Spektrum Brands, Blacksburg, VA) into ultrapure water. Additionally, the total dissolved inorganic carbon concentration was adjusted to 2,000 μmol kg<sup>-1</sup> by dissolving sodium bicarbonate into the artificial seawater. Two separate batches with distinct salinities were created (23 and 32‰) according to the in situ bottom water salinities measured during the cruise (Table S1 in Supporting Information S1). Incubation vessels, sediment, and artificial seawater were equilibrated at 5°C for ca. 16 h before starting the incubations. After adding 60 mL of artificial seawater to the sediment, the mixture was stirred into a slurry and the incubation vessels were closed with rubber septa. 25 mL of laboratory air was added as an overpressure with a syringe to prevent pressures below 1 bar after repeated sampling. Vessels were incubated in the dark in a temperature-controlled room at 5°C for 14 weeks. The slurry was shaken regularly to ensure continued oxygenation of the sediment. For all but one sample, the lowest headspace O<sub>2</sub> concentration was >8% at the end of the incubation, indicating oxic conditions. Sample 47 exhibited O<sub>2</sub> depletion (<5% O<sub>2</sub>) at the end of the incubation, so the last time point was not used.

Headspace and water samples were taken from the incubation vessels at four time points during the incubation period (1 hr, 7 days, 40 days, and 99 days). Headspace samples were taken through the septum using a gastight syringe and directly injected into an 8610C gas chromatograph (SRI Instruments, Germany). Carbon dioxide and O<sub>2</sub> were separated using a Porapak Q precolumn coupled to a HayeSep D packed column at 60°C isothermal. Target gas species were detected with a flame ionization detector (CO<sub>2</sub>) and an electron capture detector (O<sub>2</sub>). Concentrations were determined via linear regression (concentration vs. response) of standard gas mixtures ranging from 320 to 2,000 ppm CO<sub>2</sub> and 10%–21% O<sub>2</sub> (Air Liquide Gas AB, Sweden) using integrated peak area signals of the target gases. The water phase was sampled by extracting exactly 1 mL of water with a gastight syringe through a syringe filter (0.45 μm pore size). The sample was transferred into preflushed (N<sub>2</sub>) gastight glass vials and acidified with 100 μL of 85% H<sub>3</sub>PO<sub>4</sub>, converting all forms of dissolved inorganic carbon to unionized species (CO<sub>2</sub> + H<sub>2</sub>CO<sub>3</sub>). After equilibration, the headspace of the gas vial was sampled and injected into a GC-FID (above) for CO<sub>2</sub> quantification. Temperature and pressure were measured directly beforehand as supplementary parameters for calculating CO<sub>2</sub> partitioning.

The total amount of headspace CO<sub>2</sub> and O<sub>2</sub> were calculated using the ideal gas law and data on headspace concentration, pressure, and temperature for each time point. Gas solubility was calculated to derive the total amount of dissolved O<sub>2</sub> in the water phase of the incubation vessels and the amount of CO<sub>2</sub> dissolved within the water phase of the gas vials. Henry coefficients for O<sub>2</sub> were calculated based on Johnsson (2010) and for CO<sub>2</sub> based on Weiss (1974), assuming 5°C and 23‰ or 32‰ salinity, respectively. Flux rates were derived from the

slope of a linear regression of total CO<sub>2</sub> or total O<sub>2</sub> (headspace + water phase) versus the incubation time and are given in μmol g DW<sup>-1</sup> d<sup>-1</sup>. As for the shipboard incubations, both data sets are given as absolute values. Respiratory quotients were calculated using the ratio of CO<sub>2</sub> production over O<sub>2</sub> consumption.

## 2.5. Chemical and Physical Sediment Characterization

Organic carbon and nitrogen as well as δ<sup>13</sup>C of sediments were taken from a previous publication (Wild et al., 2023). Carbon and nitrogen contents are given in weight percent (wt%), and the organic carbon to nitrogen ratio (OC/N) was calculated based on molar contents. For organic carbon and nitrogen content, the uncertainty was determined based on replicates of a reference material (acetanilide) with coefficients of variation of 1.6 and 1.9, respectively. The uncertainty of δ<sup>13</sup>C was assessed by routine replicate measurements of the IAEA reference material CH7, and an in-house standard material and is estimated as 0.15‰.

Radiocarbon analysis was conducted for bulk organic carbon. An amount of sample equaling approximately 1 mg of organic carbon was weighed into silver capsules. Particulate carbonate minerals were removed by adding an excess of 1 M hydrochloric acid and letting the samples dry at 35°C for 48 hr in a drying oven. After preparation, samples were sent to the Ångström Laboratory (Uppsala University) for <sup>14</sup>C analysis via accelerator mass spectrometry. Radiocarbon data are presented as Δ<sup>14</sup>C values and used as a relative measure for comparing average organic carbon ages between sampling sites relative to the time of measurement. The δ<sup>13</sup>C and Δ<sup>14</sup>C values were used for dual-isotope source apportionment, to quantify the contribution of marine and terrestrial sources to sediment OC (see Text S3 in Supporting Information S1 for details).

Lignin phenol biomarkers were quantified from the sediment following Goñi and Montgomery (2000) with minor modifications previously described in Martens et al. (2019). Briefly, freeze-dried sediment samples were depolymerized via alkaline copper oxide oxidation, and the oxidation products were then extracted with ethyl acetate. Individual lignin phenol monomers were separated, detected, and quantified using gas chromatograph mass spectrometry. A detailed method description, including method uncertainty and a listing of all target compounds and recovery standards is given in the supplement (Text S1 in Supporting Information S1). The measured amounts of copper oxide oxidation products are given in μg per g dry weight of sample (g DW) and per 1 g organic carbon (g OC). Total lignin was calculated as the sum of syringyl, vanillyl and cinnamyl phenols in μg g<sup>-1</sup> DW and μg g<sup>-1</sup> OC. To elucidate the degradation state and origin of terrOM, several commonly used proxies were calculated. As in Matsubara et al. (2022), three degradation proxies were calculated: 3,5-dihydroxybenzoic acid over total vanillyl phenols (3,5-Bd/V), syringic acid over syringaldehyde (Sd/SI), and vanillic acid over vanillin (Vd/VI), which all positively correlate with degradation state. To investigate the origin of terrOM, two proxies were calculated: the ratio of total syringyl phenols over total vanillyl phenols (S/V) and total cinnamyl phenols over total vanillyl phenols (C/V; Jex et al., 2014).

The procedure for extraction and purification of *n*-alkanes has previously been described in Martens et al. (2020). Briefly, freeze-dried sediment was extracted with a mixture of dichloromethane and methanol, and the extracts were further fractionated in two steps. Neutral and acid soluble lipids were separated via solid-phase extraction, and the neutral lipids were then further fractionated into low-polarity (*n*-alkanes) and high-polarity (*n*-alkanols) lipids. Individual *n*-alkanes were then separated and quantified with gas chromatography mass spectrometry. A detailed method description is given in the supplements (Text S2 in Supporting Information S1). Total HMW *n*-alkane content was calculated as the sum of C25–C33 *n*-alkanes and given in μg g<sup>-1</sup> OC and μg g<sup>-1</sup> DW. This value was used as a proxy for assessing the contribution of terrOM to the sediment. The carbon preference index of HMW *n*-alkanes (CPI<sub>alk</sub>) is commonly used to assess the degradation state of terrOM (e.g., Martens et al., 2020; Wild et al., 2022) and decreases toward 1 with increasing degradation.

For grain size analysis, about 1 g of freeze-dried sediment was combusted at 400°C for 12 hr. The ash was then removed by washing the combusted samples twice with 45 mL deionized water followed by centrifugation. Finally, the washed samples were freeze-dried. Grain size analysis was conducted using a Malvern Instruments Ltd Mastersizer 3000, and the samples were introduced, circulated, and dispersed via the Hydro LV wet dispersion system. Sodium metaphosphate was added prior to each measurement as a dispersion agent. An amount of sample was added via the Hydro LV which resulted in an obscuration value between 5% and 15%. Grain size measurement was repeated 5 times per sample, and an average was calculated for further use. Grain size classes were defined as clay (<2 μm), silt (2–63 μm), and sand (>63 μm) for this study.

## 2.6. Statistics

Statistical analyses were conducted using the software IBM SPSS Statistics (version 29). Correlations between flux rates and sediment properties were tested using two-tailed Spearman's rank correlation tests due to the overall low  $n$  ( $n=16$ ) for each variable and differing distribution patterns of data sets. The null hypothesis, assuming no difference between stations, was rejected for test results exhibiting  $p < 0.05$ . Test results with  $p < 0.05$  were classified as significant, whereas test results exhibiting  $p$ -values slightly above 0.05, were classified as marginally significant ( $p > 0.05$  and  $< 0.1$ ).

## 3. Results

### 3.1. Chemical and Physical Sediment Characteristics

The measured chemical and physical sediment characteristics showed high spatial variability for several parameters. Specifically, TOC contents varied between 0.15% and 2.28% without any clear spatial trends (Figure 2a). Similarly, grain size distribution varied strongly with clay ranging between 0% and 8.6%, and silt and sand ranging between 0% and 100%, respectively (Table S2 in Supporting Information S1). Statistically significant positive (clay and silt) and negative (sand) correlations ( $p < 0.05$ ) were found between TOC and grain size (Table S11 in Supporting Information S1). Spatial trends could be observed for OC/N and  $\delta^{13}\text{C}$ . OC/N decreased from ca. 10–14 to 7–8 and  $\delta^{13}\text{C}$  increased from ca.  $-27.5\text{‰}$  to  $-24\text{‰}$  with distance to land (Figures 2b and 2g). Terrestrial biomarker contents (HMW  $n$ -alkanes and lignin phenols) showed intermediate to high values in the Kara Sea, inner Laptev Sea, and inner ESS, and lower values in the outer Laptev Sea and central ESS, both when normalized by DW and OC (Figures 2c and 2e; Table S2 in Supporting Information S1). Molecular degradation proxies suggest an increasing degradation state of terrOM with distance from land, indicated by cross-shelf gradients in  $\text{CPI}_{\text{alk}}$ , Vd/Vl, Sd/Si, and 3,5-Bd/V. For example, Vd/Vl increased from ca. 0.3–0.6 close to land to ca. 0.7–1.1 on the outer shelf and  $\text{CPI}_{\text{alk}}$  decreased from ca. 4–6 to ca. 2–3 from shore to outer shelf (Figures 2d, 2f, 2i, and 2j).

Isotopic and molecular source proxies both indicated an overall mixed organic matter composition for most samples with only slight trends for individual spatial groups. Dual carbon isotopes ( $\Delta^{14}\text{C}$  and  $\delta^{13}\text{C}$ ) have been traditionally used in the study region to investigate the origin of sediment organic matter to distinguish the different organic matter sources: active layer soil, Ice Complex deposits (present in the Laptev Sea and ESS catchments), peat deposits (abundant in the Kara Sea catchment), and marine organic matter (Martens et al., 2022; Figure S1 in Supporting Information S1). Dual-isotope source apportionment suggests that 48%–88% of the OC was derived from land sources. Differences could be observed for samples from certain spatial groups, with inner ESS samples showing the highest contribution of Ice Complex deposits (64%), outer Laptev Sea of marine organic matter (43%–52%), and Kara Sea of active layer (36%–39%) (Table S2 in Supporting Information S1).

Lignin phenols further allow to distinguish four generalized sources of vascular plant tissues: woody gymnosperm, nonwoody gymnosperm, woody angiosperm and nonwoody angiosperm tissues. Similar to the isotopic approach, lignin phenol source proxies showed a mixed composition with all samples located outside the ranges defined for pure source materials (Figure S1 in Supporting Information S1). Only sediment samples from the inner Laptev Sea exhibited slightly lower S/V and C/V values than other stations, indicating a higher contribution of material from boreal forests.

### 3.2. Shipboard O<sub>2</sub> Consumption Rates and Correlation With Sediment Characteristics

The lowest O<sub>2</sub> concentration observed during shipboard sediment core incubations was 150  $\mu\text{M}$ , indicating that conditions remained oxic throughout the experiment for all samples. All sediment cores showed significant O<sub>2</sub> uptake with two exceptions where net O<sub>2</sub> release indicated an improper seal of the lid (stations 61 and 63); O<sub>2</sub> fluxes from these stations were not used for any further analyses. Sediment O<sub>2</sub> consumption was highly variable (Figure 3a) with rates ranging between 266 and 4,981  $\mu\text{mol m}^{-2} \text{d}^{-1}$ , and no spatial trends could be observed (Table S7 in Supporting Information S1). Most consumption rates in the inner Laptev Sea and ESS ranged between ca. 1,300 and 2,500  $\mu\text{mol m}^{-2} \text{d}^{-1}$  with the exception of station 74 (266  $\mu\text{mol m}^{-2} \text{d}^{-1}$ ; Table S7 in Supporting Information S1). The highest O<sub>2</sub> consumption was measured in the outer Laptev Sea (station 47; 4,981  $\mu\text{mol m}^{-2} \text{d}^{-1}$ ), in close proximity to stations with substantially lower O<sub>2</sub> consumption rates (station 50 and 52; 652 and 1,384  $\mu\text{mol m}^{-2} \text{d}^{-1}$ ). The O<sub>2</sub> consumption rates showed significant positive correlations with clay

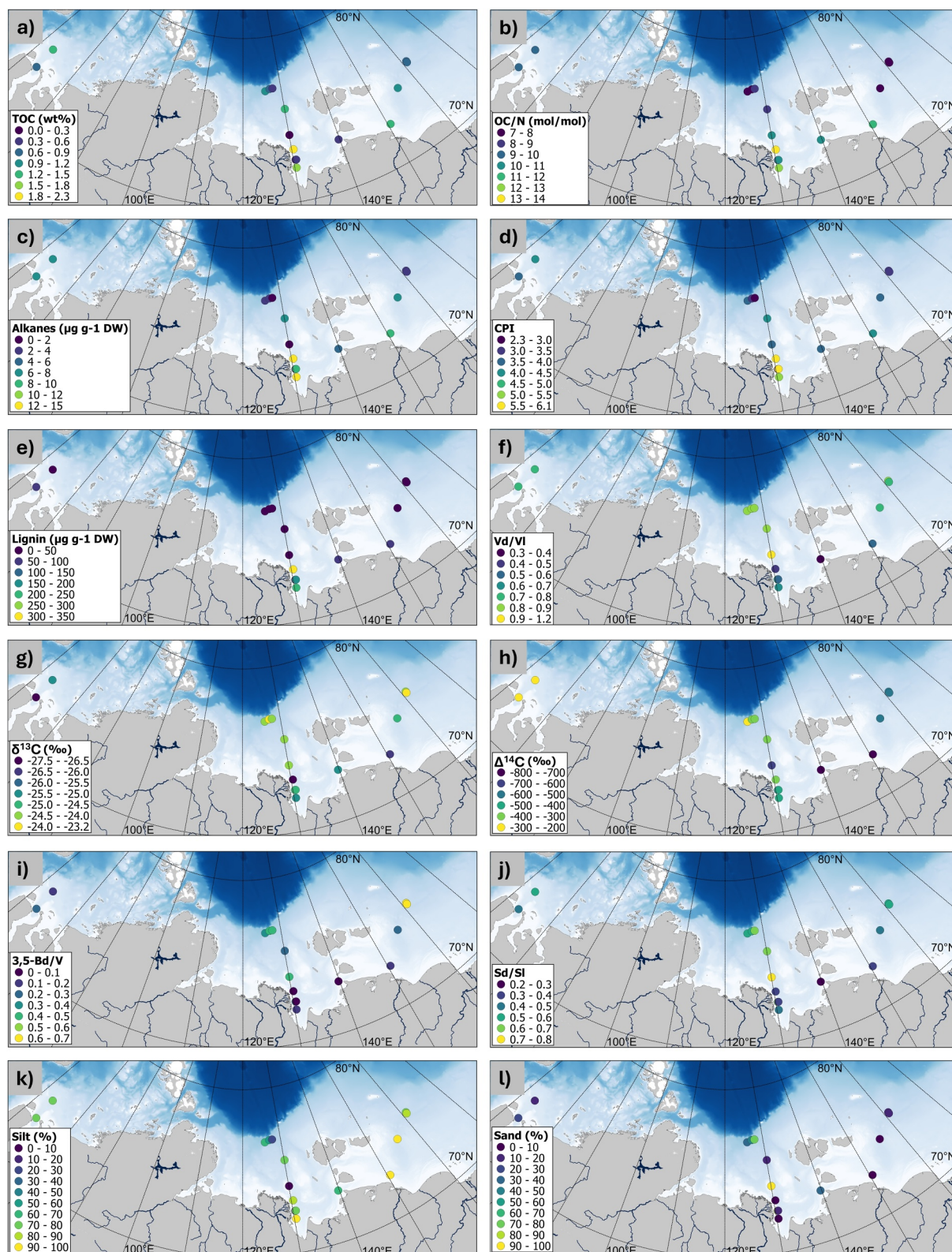


Figure 2.

content ( $\rho = 0.60$ ) and marginally significant ( $0.05 < p < 0.1$ ) positive and negative correlations with silt and sand content, respectively (silt:  $\rho = 0.47$ ; sand:  $-0.47$ ; Figure 4a). No other chemical or physical sediment characteristics significantly correlated with shipboard  $O_2$  consumption (Figure 4a, Table S8 in Supporting Information S1).

### 3.3. Slurry Incubations: $O_2$ and $CO_2$ Fluxes and Correlation With Sediment Characteristics

Potential  $O_2$  and  $CO_2$  fluxes, determined during laboratory slurry incubations, varied substantially and only showed slight spatial trends (Figures 3b and 3c; see Tables S3–S6 in Supporting Information S1 for absolute values). Within the ESS, a decrease of  $CO_2$  production and  $O_2$  consumption rates could be seen with distance to land from 0.28 to 0.06  $\mu\text{mol g}^{-1} \text{DW d}^{-1}$  and from 0.8 to 0.32  $\mu\text{mol g}^{-1} \text{DW d}^{-1}$ , respectively. This trend was linked to a gradient in OC content, and disappeared when rates were normalized by OC (Table S4 in Supporting Information S1). No spatial trends were observed in the Kara Sea and Laptev Sea. As for shipboard  $O_2$  consumption, stations with relatively high potential  $CO_2$  and  $O_2$  flux rates were located in close proximity to stations with substantially lower rates (Figures 3b and 3c; Tables S3 and S5 in Supporting Information S1). A highly significant correlation was found between potential  $CO_2$  production and  $O_2$  consumption ( $\rho = 0.84$ ;  $p < 0.001$ ), while neither correlated significantly with shipboard  $O_2$  consumption (Table S8 in Supporting Information S1).

Potential  $O_2$  and  $CO_2$  fluxes normalized by sediment DW significantly correlated with 8 and 10 out of 21 tested sediment characteristics, respectively (Figures 4b and 4c; Table S8 in Supporting Information S1). Both,  $CO_2$  production and  $O_2$  consumption were significantly correlated with TOC and TN ( $\rho = 0.59$ – $0.69$ ), and  $O_2$  consumption was marginally significantly correlated with OC/N ( $\rho = 0.43$ ). Marginally significant negative correlations were also found between both fluxes and  $\delta^{13}\text{C}$  ( $CO_2$ :  $\rho = -0.47$ ;  $O_2$ :  $\rho = -0.49$ ). A significant positive correlation was found for silt content and a negative correlation for sand content ( $CO_2$ :  $\rho = 0.67$ ,  $-0.67$ ;  $O_2$ :  $\rho = 0.51$ ,  $-0.49$ ). Both, total lignin and HMW *n*-alkane content (normalized to g DW) showed a significant positive correlation with  $CO_2$  and  $O_2$  flux; correlation coefficients ranged between 0.55 and 0.65 (Figures 4b and 4c; Table S8 in Supporting Information S1). Also, the degradation proxies 3,5Bd/V and  $\text{CPI}_{\text{alk}}$  exhibited significant negative and positive correlations with both fluxes, respectively. Thus, both indicate higher fluxes with lower degradation state. Other degradation proxies also showed marginally significant correlations, Vd/Vl correlating with  $CO_2$  production ( $\rho = -0.49$ ) and Sd/SI with  $O_2$  consumption ( $\rho = -0.43$ ; Table S8 in Supporting Information S1). The terrOM source proxies S/V and C/V, as well as  $\Delta^{14}\text{C}$  and water depth, did not correlate with either  $CO_2$  production or  $O_2$  consumption (Table S8 in Supporting Information S1).

We additionally explored correlations of  $O_2$  and  $CO_2$  fluxes normalized by sediment OC, with sediment parameters. These correlations offer insights into how OC quality rather than quantity influences decomposition. Rates of  $CO_2$  production were only marginally significantly correlated with silt ( $\rho = 0.44$ ) and Sd/SI ( $\rho = -0.45$ ); no other significant correlations were observed. Rates of  $O_2$  consumption did not show significant correlations.

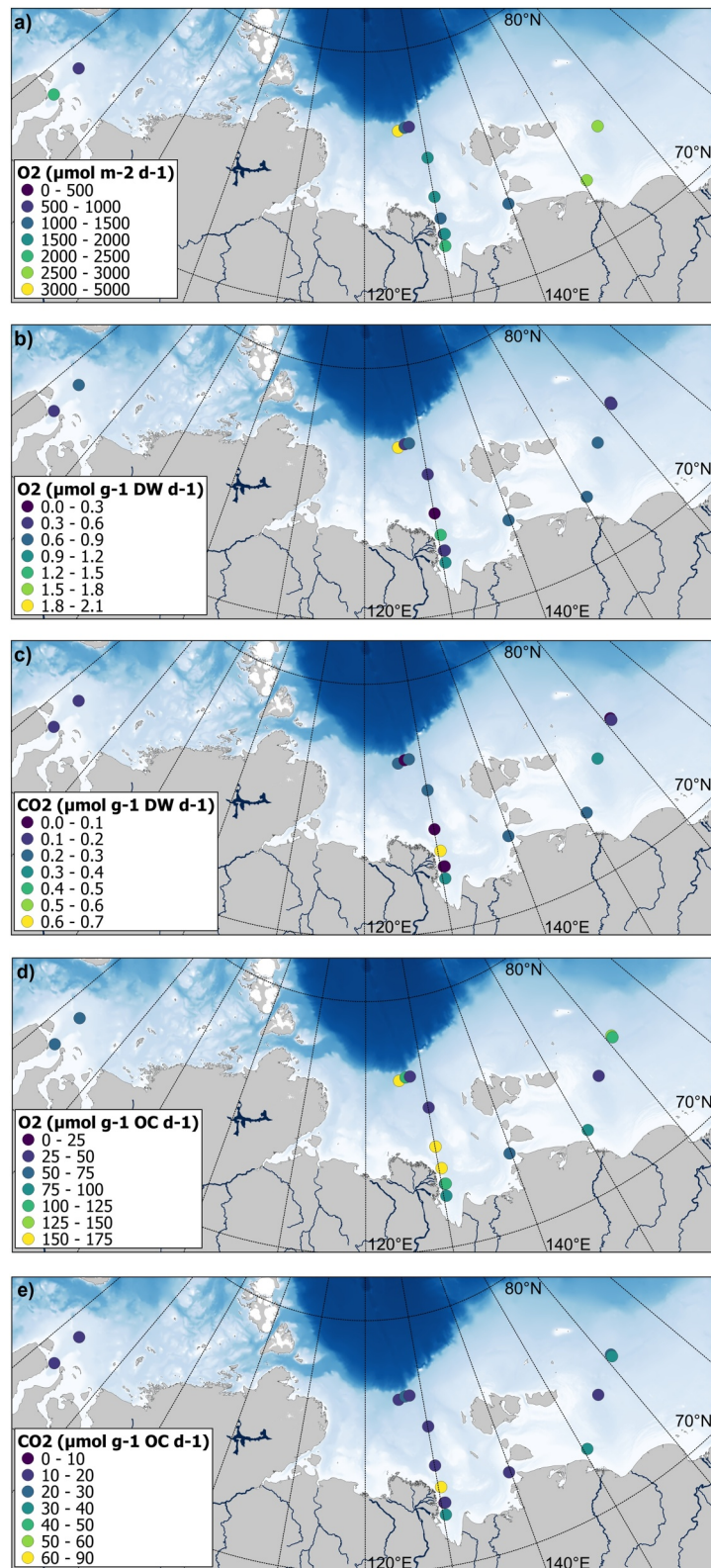
Although both  $O_2$  consumption and  $CO_2$  production rates exhibited similar variability between sites and showed a strong correlation with each other, absolute  $O_2$  consumption was consistently at least twice as high as  $CO_2$  production for a given site (Figures 3b and 3c). The  $O_2$  consumption ranged between 0.24 and 1.94  $\mu\text{mol g}^{-1} \text{DW d}^{-1}$ , whereas  $CO_2$  production ranged between 0.03 and 0.67  $\mu\text{mol g}^{-1} \text{DW d}^{-1}$ . Resulting respiratory quotients, calculated as the ratio of  $CO_2$  production over  $O_2$  consumption, were below 0.51 for all sites with values varying between 0.11 and 0.51 (Figure 5).

## 4. Discussion

### 4.1. Potential $O_2$ Consumption and $CO_2$ Production: Drivers of Variability

To assess the potential for aerobic organic matter degradation of different surface sediments,  $O_2$  and  $CO_2$  fluxes were determined using sediment slurry incubations. Due to the artificial setup of the experiment, which included

**Figure 2.** Surface plots of selected sediment properties across the interior Siberian shelf seas. Sediment properties of following parameters are depicted in panels (a) total organic carbon content (TOC), (b) organic carbon to nitrogen ratio (OC/N), (c) sum of C25–C33 *n*-alkanes, (d) their carbon preference index (CPI), (e) sum of syringyl, vanillyl, and cinnamyl phenols (lignin), (f) the ratio of vanillic acid over vanillin (Vd/Vl), (g)  $\delta^{13}\text{C}$ , (h)  $\Delta^{14}\text{C}$ , (i) 3,5-dihydroxybenzoic acid over total vanillyl phenols (3,5Bd/V), (j) syringic acid over syringaldehyde (Sd/SI), and (k and l) relative amounts of silt and sand from total mineral particles in percent. Bathymetric data of IBCAO version 4 (Jakobsson et al., 2020) is used as the background map.

**Figure 3.**

frequent mixing, full oxygenation, dark conditions, no in- or outflow of water or sediment, and the exclusion of Arctic seawater microbial communities, the determined flux values are not directly transferrable to in situ conditions. Instead, these fluxes reflect the potential of organic matter to be mineralized under aerobic conditions and aid in our understanding of the mechanisms that regulate in situ processes.

Rates of CO<sub>2</sub> production observed in this experiment were highly variable, but overall comparable in magnitude to previous observations from the region. A previous slurry incubation study measured aerobic CO<sub>2</sub> production between 15.6 and 73.4 μmol g OC<sup>-1</sup> d<sup>-1</sup> for the eastern ESS (Karlsson et al., 2015), which is comparable to the range measured in this study in the Kara Sea, Laptev Sea, and western ESS (7.9–88.6 μmol g OC<sup>-1</sup> d<sup>-1</sup>). It is necessary to highlight that geographical focus and incubation temperature differ compared to our study. The previous study reported only anaerobic CO<sub>2</sub> production rates for the Laptev Sea, which ranged between –0.002 and 3.8 μmol g OC<sup>-1</sup> d<sup>-1</sup> (6.5–24 μmol g OC<sup>-1</sup> d<sup>-1</sup> for the eastern ESS) (Karlsson et al., 2015). These anaerobic fluxes were lower than our CO<sub>2</sub> production values, which would be expected because anaerobic organic matter decomposition is known to be ca. 3 times lower than aerobic (Knoblauch et al., 2018). Potential O<sub>2</sub> consumption exhibited similar variability to CO<sub>2</sub> production in our study, but comparable values from previous experiments are lacking.

The correlations of potential CO<sub>2</sub> production and O<sub>2</sub> consumption rates with sediment properties, together with the understanding of dominant carbon sources to these sediments, suggest a strong contribution of terrOM to CO<sub>2</sub> production from surface sediments on the Siberian Arctic Ocean shelves. First, significant positive correlations of CO<sub>2</sub> production with TOC and TN indicate that organic matter content is the main driver of CO<sub>2</sub> production. This is in line with expectations, since organic matter constitutes the basis for heterotrophic respiration. Second, isotope-based source apportionment suggests that terrOM accounts for 48%–88% of TOC in surface sediments of the study area. The lack of correlation between CO<sub>2</sub> production normalized by OC and terrOM proxies indicates that terrOM has neither a higher nor a lower degradability compared to bulk organic matter. Thus, as for marine organic matter, a large portion of terrOM is labile and readily degraded in the marine environment. Taken together, these observations point at a strong contribution of terrOM to CO<sub>2</sub> production from surface sediments on the Siberian Arctic Ocean shelves. This conclusion is further supported by the significant positive correlations of DW-normalized CO<sub>2</sub> production with the amount of terrOM (DW-normalized lignin and *n*-alkane contents, δ<sup>13</sup>C, OC/N) and negative correlations with terrOM degradation state (i.e., CPI<sub>alk</sub>; Vd/VI; Figures 4b and 4c). The TOC content thus determines the potential for CO<sub>2</sub> production, and terrOM contributes a large part of the TOC in this region.

Similar correlation patterns between CO<sub>2</sub> fluxes and terrestrial biomarkers (lignin phenols and lipid biomarker) were also found in the previous study investigating aerobic and anaerobic CO<sub>2</sub> production in Laptev Sea sediments (Karlsson et al., 2015). Therein, correlations were either weaker or not present for sediments from the eastern ESS. The eastern ESS represents a marine shelf system that is more strongly influenced by Pacific water inflow and a dominance of marine organic matter, rather than terrOM (Semiletov et al., 2005). A similar trend can be observed in our data set when calculating (DW-normalized) correlation coefficients separately for outer shelf samples (central ESS + outer Laptev Sea) and inner shelf samples (inner ESS + inner Laptev Sea + Kara Sea). Both, CO<sub>2</sub> production and O<sub>2</sub> consumption showed higher correlation coefficients with the amount and degradation state of terrOM in the inner shelf sea than all stations; these proxies also rapidly changed with distance from shore within the inner shelf. By contrast, the outer shelf sediments showed limited variability in terrOM proxies, and CO<sub>2</sub> production as well as O<sub>2</sub> consumption did not correlate significantly with any of them (Tables S9 and S10 in Supporting Information S1). This indicates that interior shelf sediments in close proximity to land might exhibit a unique biogeochemical regime that is strongly influenced by deposition and degradation of terrOM.

Considering the results of this study together with previous work suggests that CO<sub>2</sub> production from terrOM declines rapidly once the terrOM enters the Arctic Ocean. Aerobic incubations of Ice Complex deposit material,

---

**Figure 3.** Surface plots of sediment gas fluxes. Sediment O<sub>2</sub> consumption rates (in μmol m<sup>-2</sup> d<sup>-1</sup>) were measured during shipboard incubations of intact sediment cores with overlying bottom water, and were originally published in Wild et al. (2023) (panel a). Potential O<sub>2</sub> consumption and potential CO<sub>2</sub> production were measured during aerobic sediment slurry incubations of surface sediments from the same sites and are shown normalized to gram dry weight sediment (in μmol g<sup>-1</sup> DW d<sup>-1</sup>, panels b and c) and normalized to gram organic carbon (in μmol g<sup>-1</sup> OC d<sup>-1</sup>, panels d and e). Fluxes were determined for samples from the Kara Sea, Laptev Sea, and western East Siberian Sea. Bathymetric data of IBCAO version 4 (Jakobsson et al., 2020) are used as the background map.

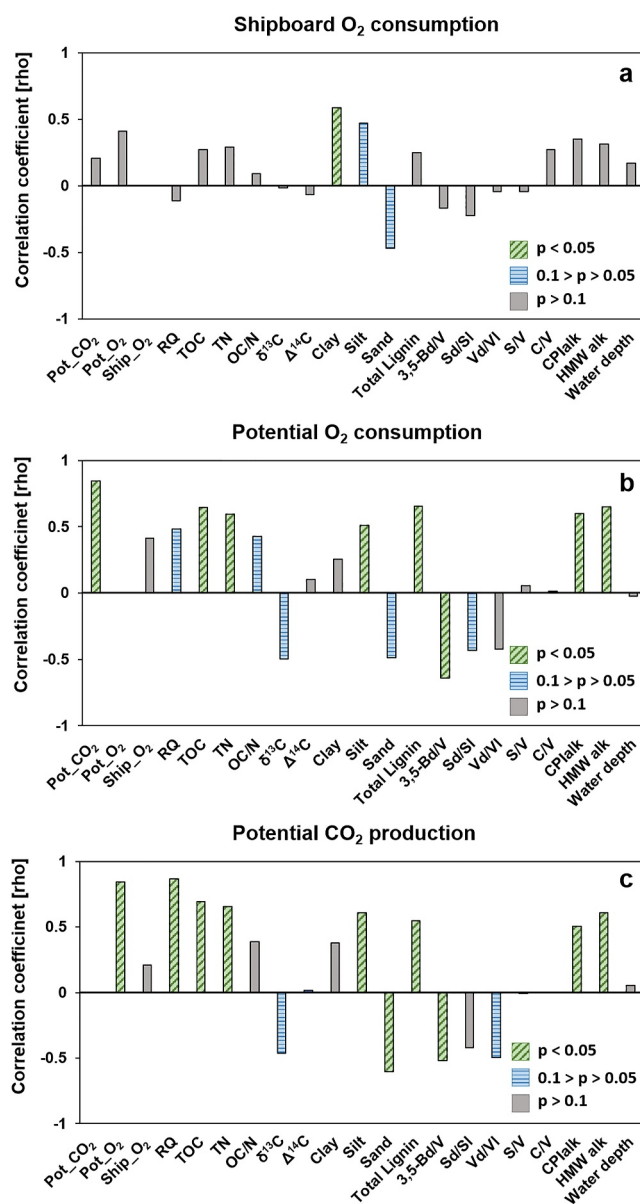


**Figure 4.** Correlations between shipboard sediment  $O_2$  consumption (Ship\_ $O_2$ , panel a), potential  $O_2$  consumption (Pot\_ $O_2$ , panel b), potential  $CO_2$  production (Pot\_ $CO_2$ , panel c), and sediment properties. The Spearman correlation coefficient ( $\rho$ ) for each flux versus sediment property parameters is plotted on the y-axis. The height of each column represents the magnitude of  $\rho$  for each parameter. The colors of bars indicate three different classes of significance for correlation coefficients: gray = not significant ( $p > 0.1$ ); blue with horizontal lines = marginally significant ( $0.1 > p > 0.05$ ); and green with diagonal lines = significant ( $p < 0.05$ ). Selected sediment parameters include total organic carbon (TOC, in wt%), total nitrogen (TN, in wt%), organic carbon to nitrogen ratio (OC/N),  $\delta^{13}C$  (‰-VPDB),  $\Delta^{14}C$  (‰), grain size fractions (clay, silt, and sand, in %), total lignin content ( $\mu\text{g g}^{-1}$  DW), ratio of 3,5-dihydroxybenzoic acid to vanillyl phenols (3,5-Bd/V), ratio of syringic acid to syringaldehyde (Sd/SI), ratio of vanillic acid to vanillin (Vd/Vl), ratio of syringyl to vanillyl phenols (S/V), ratio of cinnamyl to vanillyl phenols (C/V), carbon preference index of C25–C31 *n*-alkanes (CPI<sub>alk</sub>), sum of C25–C33 *n*-alkanes ( $\mu\text{g g}^{-1}$  DW), and water depth (m). Concentrations and fluxes are normalized by sediment dry weight; see Table S8 in Supporting Information S1 for correlations normalized by organic carbon.

collected from debris near a permafrost cliff, in seawater showed a rapid decrease in  $CO_2$  production rates during 60 days of incubation, by ca. 90% (from  $7.46 \pm 2.26$  to  $0.67 \pm 0.15 \mu\text{mol CO}_2 \text{ g DW}^{-1} \text{ d}^{-1}$ ) for comparatively fresh Ice Complex deposit material, and by ca. 50% (from  $1.09 \pm 0.11$  to  $0.54 \pm 0.03 \mu\text{mol CO}_2 \text{ g DW}^{-1} \text{ d}^{-1}$ ) for more degraded material (Tanski et al., 2021). In comparison,  $CO_2$  production rates of our stations with highest

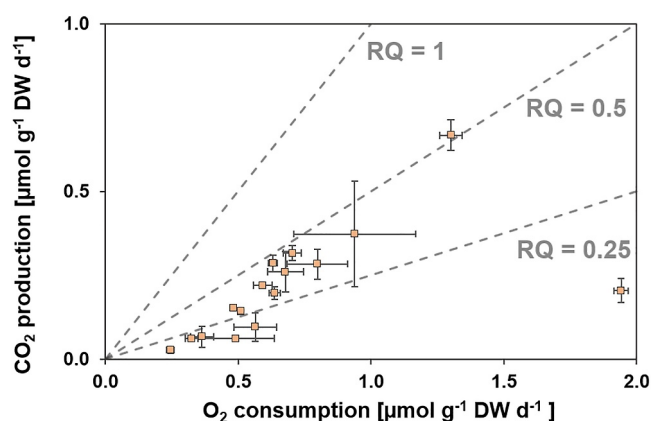


**Figure 5.** Relation between potential  $\text{CO}_2$  production and potential  $\text{O}_2$  consumption. Potential  $\text{CO}_2$  production (y-axis, in  $\mu\text{mol g}^{-1} \text{DW d}^{-1}$ ) and potential  $\text{O}_2$  consumption (x-axis, in  $\mu\text{mol g}^{-1} \text{DW d}^{-1}$ ) were measured in sediment slurry incubations for 16 stations in the Kara Sea, Laptev Sea, and western East Siberian Sea. Orange squares represent mean values ( $n = 3$ ), and error bars show the standard deviation of each data point. The three light-gray dashed lines indicate theoretical respiratory quotient (RQ) trajectories for  $\text{RQ} = 1$ ,  $\text{RQ} = 0.5$ , and  $\text{RQ} = 0.25$ , as reference values to the data points.

99 days of our aerobic incubation, samples lost on average  $3 \pm 2\%$  of the initial OC (range 1%–11%). This would result in 11% OC loss over 1 year at constant decomposition rates. Rates will however likely decline over longer time frames than our incubation as the most easily degradable substrates are depleted, as is often observed in incubations. Although these uncertainties limit robust estimates of  $\text{CO}_2$  production under in situ conditions, it seems possible that some tens of percent of OC could be lost as  $\text{CO}_2$  by aerobic decomposition in surface sediments.

Even though  $\text{CO}_2$  production and  $\text{O}_2$  consumption showed a strong relationship, the ratio between both fluxes expressed as respiratory quotients exhibited high variability between 0.11 and 0.51 (Figure 5). This range is substantially lower than in situ respiratory quotient (RQ) values determined for a wide range of different sediments, with ratios between 0.69 and 1.31 (Jørgensen et al., 2022). High RQ variability at small spatial scales was also observed in other areas, for instance, in a shallow fjord in NE Greenland where RQ values spanned from ca. 0.5 to above 1 (Glud et al., 2002). Incubations of outer Laptev Sea and ESS sediment cores yielded respiratory quotients close to 1 (0.96–1.00;  $n = 3$ ; Brüchert et al., 2018). The discrepancy to RQ values measured in our study may be explained by relatively high  $\text{O}_2$  fluxes in our laboratory slurry incubations. These might have been caused by processes not directly related to organic matter degradation. One possible process could be the reoxidation of reduced electron acceptors, such as ammonium, iron, and sulphides, which would increase the consumption of  $\text{O}_2$  without directly affecting  $\text{CO}_2$  production. The RQ values determined in this study should consequently be taken as an indication of the relationship of  $\text{CO}_2$  production and  $\text{O}_2$  consumption during the laboratory slurry incubation, but not interpreted as a realistic approximation of the in situ relationship between  $\text{CO}_2$  and  $\text{O}_2$  fluxes.

#### 4.2. Variability of Shipboard $\text{O}_2$ Consumption

Sediment  $\text{O}_2$  consumption, measured for 14 stations during shipboard sediment core incubations, showed strong spatial variability and exhibited values at the lower end of previous investigations of Arctic shelf seas. The  $\text{O}_2$  consumption averaged  $1,759 \pm 1,146 \mu\text{mol m}^{-2} \text{d}^{-1}$  across the entire study area (Figure 3a), compared to average values of  $6,200 \pm 5,600 \mu\text{mol m}^{-2} \text{d}^{-1}$  reported for interior Arctic shelf seas in a previous meta-analysis (Bourgeois et al., 2017). Specifically for the Laptev Sea, previous studies found a similarly high  $\text{O}_2$  consumption variability with rates ranging between 70 and  $13,430 \mu\text{mol m}^{-2} \text{d}^{-1}$  and decreasing with water depth (Boetius & Damm, 1998; Brüchert et al., 2018; Clough et al., 2005; Wollenburg & Kuhnt, 2000).

(>60%) Ice Complex deposit contribution in the inner ESS (Figure S1 in Supporting Information S1), were about half ( $0.28$  and  $0.26 \mu\text{mol CO}_2 \text{g DW}^{-1} \text{d}^{-1}$ ) that of the final flux rates of the reference study by Tanski et al. (2021). Taken together, these data suggest that the most easily degradable fraction of Ice Complex deposits is rapidly decomposed as it enters the seawater, and that decomposition continues at slower rates over longer time frames in the water column and the sediment. Thus, terrOM inputs are likely to contribute to  $\text{CO}_2$  production from both the water column and sediment near the shore.

Rates of  $\text{CO}_2$  production during our aerobic slurry incubation represent the potential degradability of organic matter under the incubation conditions, and cannot be directly translated to the field. Nevertheless, comparing these rates with OC burial rates and  $\text{O}_2$  penetration depths allows to put our data into context. Mass accumulation rates on the outer Laptev Sea and western East Siberian Sea shelf are in the order of  $0.15$ – $0.25 \text{g cm}^{-2} \text{yr}^{-1}$ , or  $0.10$ – $0.17 \text{cm yr}^{-1}$  (Martens et al., 2022) assuming an average bulk density of  $1.5 \text{g cm}^{-3}$  (see Table S1 in Supporting Information S1). Oxygen penetration depth in that area is ca.  $0.5$ – $1.5 \text{cm}$  (Brüchert et al., 2018); based on these assumptions, the sediment OC remains within the oxic sediment layer for 3–15 years. This time will be substantially shorter on the inner shelves, where mass accumulation rates are 2–3 times higher (Martens et al., 2022), and  $\text{O}_2$  penetration depth is unquantified but likely lower. During the

The lower rates observed in our study compared to published studies could be related to the seasonal timing of O<sub>2</sub> consumption measurements, differing research areas, and methodological differences. First, O<sub>2</sub> consumption rates in our study were measured during October, which is later in the year than most values reported in previous studies that dominantly were conducted in spring or summer (Bourgeois et al., 2017). Even though O<sub>2</sub> consumption rates encompassing several seasons are very rare, there are indications of O<sub>2</sub> consumption rates peaking in late spring or summer, likely tied to phytoplankton blooms and increased river discharge (Ardyna et al., 2013; Feng et al., 2021). Supporting this, previous studies reported higher sediment O<sub>2</sub> consumption rates during June–July in the Laptev Sea (Brüchert et al., 2018; Clough et al., 2005), than the rates presented here for October. These differences might indicate strong seasonal variability of O<sub>2</sub> consumption, highlighting that point measurements of sediment O<sub>2</sub> consumption should not be considered representative for the entire open water season. Second, most of the existing O<sub>2</sub> consumption data for Arctic Ocean shelves were measured in the Beaufort Sea; to our knowledge, only four publications reported values for the Laptev Sea and one for the ESS and no data have been published for the Kara Sea (Bourgeois et al., 2017; Brüchert et al., 2018). The circum-Arctic shelf seas differ in sedimentary and hydrological regimes, which may lead to geographical differences in overall organic matter degradability and O<sub>2</sub> consumption. Additionally, it is noteworthy that O<sub>2</sub> consumption has been measured using various methods, which all have systematic biases that affect the comparability of the results. In situ measurements generally yield the highest estimate of O<sub>2</sub> consumption, whereas ex situ measurements such as in our study in general yield lower estimates (Jørgensen et al., 2022).

Previous research suggests that for the Arctic Ocean, sediment O<sub>2</sub> consumption is primarily constrained by labile organic matter input and water depth (Bourgeois et al., 2017). In contrast to our hypothesis, we found no statistically significant relationship between shipboard O<sub>2</sub> consumption and water depth, TOC or amount and degradation state of terrOM (Figure 4a). Water depth can be seen as a proxy for the spatial and temporal separation between organic matter source and the sediment, which in turn can affect the amount and degradation state of organic matter reaching the sediment (Matsubara et al., 2022). This is supported by observations showing decreasing O<sub>2</sub> consumption with water depth from shallow shelf to slope sediments in the Laptev Sea (Clough et al., 2005). Such a relationship was not observed in our study, likely because all our stations were located on shelves, with a weak gradient in water depth (14–74 m). This may indicate that water depth is less important for constraining O<sub>2</sub> consumption on the shallow parts of the Siberian shelf seas. The lack of relationship of sediment O<sub>2</sub> consumption with parameters indicative of TOC availability, including TOC content, terrOM proxies, and potential CO<sub>2</sub> production, suggests that other factors overlay the contribution of aerobic organic matter decomposition on in situ O<sub>2</sub> consumption, such as the reoxidation of reduced compounds of iron, manganese, and sulphide.

### 4.3. Implications for Arctic Ocean Shelf Biogeochemistry

Terrigenous organic matter contributes to total sedimentary organic matter content, and to sediment CO<sub>2</sub> fluxes in the Siberian Shelf seas. For near-coastal shelf seas, the dominance of terrOM inputs (Belicka et al., 2002; Martens et al., 2022) might be an important driver of organic matter mineralization and associated CO<sub>2</sub> production and O<sub>2</sub> consumption, rather than marine organic matter. Combining our findings with previous studies on the decomposition of coastal Ice Complex deposits suggests that part of terrOM that is eroded on land and deposited into shelf sediments is transformed back to CO<sub>2</sub>. During summer months when substantial freshwater discharge leads to strong stratification of Siberian shelf seawaters (Osadchiev, Frey, Shchuka, et al., 2021; Osadchiev, Frey, Spivak, et al., 2021), CO<sub>2</sub> released from sediments can accumulate in bottom waters, leading to a decrease in bottom water pH (Semiletov et al., 2016). Our findings support previous suggestions that terrOM decomposition may add to seasonal bottom water acidification in Arctic Ocean shelf seas, which could have cascading effects on Arctic Ocean biogeochemistry and food webs. However, this stratification is disrupted during winter months because of decreased freshwater discharge and storms. Thus, CO<sub>2</sub> produced by terrOM degradation that exceeds the partial pressure of the atmosphere will be vented into the atmosphere once the stratification is disrupted and thereby contributes to the permafrost carbon feedback, exacerbating climate change.

### Data Availability Statement

All data are included in the Supporting Information S1 and additionally deposited in the publicly available Bolin Centre Database (Sauerland et al., 2024, <https://doi.org/10.17043/sauerland-2024-arctic-sediments-1>).

### Acknowledgments

We thank the scientific team and the crew of the ISSS-2020 expedition, as well as Draupnir Einarsson (Stockholm University) for developing the core incubation setup. The work was funded by the Swedish Research Council VR (Grants 2018-05489 and 2021-01750 to B.W., 2021-06670 to J.M., and 2017-01601 to Ö. G.), the Swedish Research Council for Sustainable Development (Formas) (Grant 2018-01547 to B.W.), the Carl Trygger Foundation (Grant CTS 20: 470 to B.W.) and the European Research Council (ERC-AdG CC-Top, Grant 695331 to Ö.G.). The field work was supported by the Russian Science Foundation (Grant 21-77-30001 to I.S.), with additional support from the Ministry of Science and Higher Education of the Russian Federation (Grant “Priority-2030”, SakhGU and by Grant FEFF-2024-0004, SakhGU). The ship charter of the R/V Akademik Mstislav Keldysh was funded by Grant 121021500057-4 (POI), and by Grant “Priority-2030” (TGU) from the Ministry of Science and Higher Education of the Russian Federation.

### References

- Ardyna, M., Babin, M., Gosselin, M., Devred, E., Bélanger, S., Matsuoka, A., & Tremblay, J.-É. (2013). Parameterization of vertical chlorophyll *a* in the Arctic Ocean: Impact of the subsurface chlorophyll maximum on regional, seasonal, and annual primary production estimates. *Biogeosciences*, 10(6), 4383–4404. <https://doi.org/10.5194/bg-10-4383-2013>
- Belicka, L. L., Macdonald, R. W., & Harvey, H. (2002). Sources and transport of organic carbon to shelf, slope, and basin surface sediments of the Arctic Ocean. *Deep Sea Research Part I: Oceanographic Research Papers*, 49(8), 1463–1483. [https://doi.org/10.1016/S0967-0637\(02\)00031-6](https://doi.org/10.1016/S0967-0637(02)00031-6)
- Boetius, A., & Damm, E. (1998). Benthic oxygen uptake, hydrolytic potentials and microbial biomass at the Arctic continental slope. *Deep Sea Research Part I: Oceanographic Research Papers*, 45(2–3), 239–275. [https://doi.org/10.1016/S0967-0637\(97\)00052-6](https://doi.org/10.1016/S0967-0637(97)00052-6)
- Bourgeois, S., Archambault, P., & Witte, U. (2017). Organic matter remineralization in marine sediments: A Pan-Arctic synthesis. *Global Biogeochemical Cycles*, 31(1), 190–213. <https://doi.org/10.1002/2016GB005378>
- Brüchert, V., Bröder, L., Sawicka, J. E., Tesi, T., Joye, S. P., Sun, X., et al. (2018). Carbon mineralization in Laptev and East Siberian sea shelf and slope sediment. *Biogeosciences*, 15(2), 471–490. <https://doi.org/10.5194/bg-15-471-2018>
- Capelle, D. W., Kuzyk, Z. Z. A., Papakyriakou, T., Guéguen, C., Miller, L. A., & Macdonald, R. W. (2020). Effect of terrestrial organic matter on ocean acidification and CO<sub>2</sub> flux in an Arctic shelf sea. *Progress in Oceanography*, 185, 102319. <https://doi.org/10.1016/j.pocean.2020.102319>
- Crough, L. M., Renaud, P. E., & Ambrose, W. G., Jr. (2005). Impacts of water depth, sediment pigment concentration, and benthic macrofaunal biomass on sediment oxygen demand in the western Arctic Ocean. *Canadian Journal of Fisheries and Aquatic Sciences*, 62(8), 1756–1765. <https://doi.org/10.1139/f05-102>
- Feng, D., Gleason, C. J., Lin, P., Yang, X., Pan, M., & Ishitsuka, Y. (2021). Recent changes to Arctic river discharge. *Nature Communications*, 12(1), 6917. <https://doi.org/10.1038/s41467-021-27228-1>
- Fuchs, M., Nitze, I., Strauss, J., Günther, F., Wetterich, S., Kizyakov, A., et al. (2020). Rapid fluvio-thermal erosion of a yedoma permafrost cliff in the Lena River Delta. *Frontiers in Earth Science*, 8, 336. <https://doi.org/10.3389/feart.2020.00336>
- Glud, R. N., Kühl, M., Wenzhöfer, F., & Rysgaard, S. (2002). Benthic diatoms of a high Arctic fjord (young sound, NE Greenland): Importance for ecosystem primary production. *Marine Ecology Progress Series*, 238, 15–29. <https://doi.org/10.3354/meps238015>
- Goñi, M. A., & Montgomery, S. (2000). Alkaline CuO oxidation with a microwave digestion system: Lignin analyses of geochemical samples. *Analytical Chemistry*, 72(14), 3116–3121. <https://doi.org/10.1021/ac991316w>
- Gordeev, V. V. (2000). River input of water, sediment, major ions, nutrients and trace metals from Russian territory to the Arctic Ocean. In *The freshwater budget of the Arctic Ocean* (pp. 297–322). Springer. [https://doi.org/10.1007/978-94-011-4132-1\\_14](https://doi.org/10.1007/978-94-011-4132-1_14)
- Gustafsson, Ö., van Dongen, B. E., Vonk, J. E., Dudarev, O. V., & Semiletov, I. P. (2011). Widespread release of old carbon across the Siberian Arctic echoed by its large rivers. *Biogeosciences*, 8(6), 1737–1743. <https://doi.org/10.5194/bg-8-1737-2011>
- Holmes, R. M., McClelland, J. W., Peterson, B. J., Shiklomanov, I. A., Shiklomanov, A. I., Zhulidov, A. V., et al. (2002). A circumpolar perspective on fluvial sediment flux to the Arctic ocean. *Global Biogeochemical Cycles*, 16(4), 1098. <https://doi.org/10.1029/2001GB001849>
- Hugelius, G., Loisel, J., Chadburn, S., Jackson, R. B., Jones, M., MacDonald, G., et al. (2020). Large stocks of peatland carbon and nitrogen are vulnerable to permafrost thaw. *Proceedings of the National Academy of Sciences of the United States of America*, 117(34), 20438–20446. <https://doi.org/10.1073/pnas.1916387117>
- Jakobsson, M., Grantz, A., Kristoffersen, Y., & Macnab, R. (2003). Physiographic provinces of the Arctic Ocean seafloor. *GSA Bulletin*, 115(12), 1443. <https://doi.org/10.1130/B25216.1>
- Jakobsson, M., Mayer, L. A., Bringensparr, C., Castro, C. F., Mohammad, R., Johnson, P., et al. (2020). The international bathymetric chart of the Arctic Ocean version 4.0. *Scientific Data*, 7(1), 176. <https://doi.org/10.1038/s41597-020-0520-9>
- Jex, C. N., Pate, G. H., Blyth, A. J., Spencer, R. G., Hernes, P. J., Khan, S. J., & Baker, A. (2014). Lignin biogeochemistry: From modern processes to quaternary archives. *Quaternary Science Reviews*, 87, 46–59. <https://doi.org/10.1016/j.quascirev.2013.12.028>
- Johnson, M. T. (2010). A numerical scheme to calculate temperature and salinity dependent air-water transfer velocities for any gas. *Ocean Science*, 6(4), 913–932. <https://doi.org/10.5194/os-6-913-2010>
- Jones, B. M., Irrgang, A. M., Farquharson, L. M., Lantuit, H., Whalen, D., Ogorodov, S., et al. (2020). *Arctic report card 2020: Coastal permafrost erosion*. United States. National Oceanic and Atmospheric Administration. Office of Oceanic and Atmospheric Research University of Alaska Fairbanks. Institute of Northern Engineering Alfred-Wegener-Institut für Polar- und Meeresforschung / Alfred Wegener Institute, Helmholtz Centre for Polar and Marine Research University of Alaska (College). Geophysical Institute Geological Survey of Canada (Atlantic) Moskovskii gosudarstvennyi universitet im. M.V. Lomonosova / Lomonosov Moscow State University Institut zemnoi kory (Rossiiskai`a` akademii`a` nauk) / Siberian Branch, Russian Academy of Sciences University of Texas at El Paso Geological Survey (U.S.) Uniwersytet Wrocławski / University of Wrocław SINTEF-gruppen (Norway) Københavns universitet / University of Copenhagen Universidade de Lisboa. Instituto de Geografia e Ordenamento do Território / Institute of Geography and Spatial Planning, University of Lisbon Universität Potsdam. Institut für Geographie und Geoökologie / Institute of Geosciences University of Potsdam University of Alaska Fairbanks. Geophysical Institute Alaska. Division of Geological and Geophysical Surveys University of Colorado (Boulder campus). Institute of Arctic and Alpine Research Uniwersytet Marii Curie-Skłodowskiej / Marie Curie Skłodowska University. Retrieved from <https://repository.library.noaa.gov/view/noaa/27897>
- Jørgensen, B. B., Wenzhöfer, F., Egger, M., & Glud, R. N. (2022). Sediment oxygen consumption: Role in the global marine carbon cycle. *Earth-Science Reviews*, 228, 103987. <https://doi.org/10.1016/j.earscirev.2022.103987>
- Karlsson, E. S., Brüchert, V., Tesi, T., Charin, A., Dudarev, O., Semiletov, I., & Gustafsson, Ö. (2015). Contrasting regimes for organic matter degradation in the East Siberian Sea and the Laptev Sea assessed through microbial incubations and molecular markers. *Marine Chemistry*, 170, 11–22. <https://doi.org/10.1016/j.marchem.2014.12.005>
- Knoblauch, C., Beer, C., Liebner, S., Grigoriev, M. N., & Pfeiffer, E.-M. (2018). Methane production as key to the greenhouse gas budget of thawing permafrost. *Nature Climate Change*, 8(4), 309–312. <https://doi.org/10.1038/s41558-018-0095-z>
- Lantuit, H., Overduin, P. P., Couture, N., Wetterich, S., Aré, F., Atkinson, D., et al. (2012). The Arctic coastal dynamics Database: A New classification scheme and Statistics on Arctic permafrost coastlines. *Estuaries and Coasts*, 35(2), 383–400. <https://doi.org/10.1007/s12237-010-9362-6>
- Martens, J., Wild, B., Muschitiello, F., O’Regan, M., Jakobsson, M., Semiletov, I., et al. (2020). Remobilization of dormant carbon from Siberian-Arctic permafrost during three past warming events. *Science Advances*, 6(42), eabb6546. <https://doi.org/10.1126/sciadv.abb6546>
- Martens, J., Wild, B., Pearce, C., Tesi, T., Andersson, A., Bröder, L., et al. (2019). Remobilization of old permafrost carbon to chukchi Sea Sediments during the end of the last deglaciation. *Global Biogeochemical Cycles*, 33(1), 2–14. <https://doi.org/10.1029/2018GB005969>
- Martens, J., Wild, B., Semiletov, I., Dudarev, O. V., & Gustafsson, Ö. (2022). Circum-Arctic release of terrestrial carbon varies between regions and sources. *Nature Communications*, 13(1), 5858. <https://doi.org/10.1038/s41467-022-33541-0>

- Matsubara, F., Wild, B., Martens, J., Andersson, A., Wennström, R., Bröder, L., et al. (2022). Molecular-multiproxy assessment of land-derived organic matter degradation over extensive scales of the East Siberian Arctic shelf seas. *Global Biogeochemical Cycles*, 36(12), e2022GB007428. <https://doi.org/10.1029/2022GB007428>
- Nielsen, D. M., Pieper, P., Barkhordarian, A., Overduin, P., Ilyina, T., Brovkin, V., et al. (2022). Increase in Arctic coastal erosion and its sensitivity to warming in the twenty-first century. *Nature Climate Change*, 12(3), 263–270. <https://doi.org/10.1038/s41558-022-01281-0>
- Osadchiev, A., Frey, D., Spivak, E., Shchuka, S., Tilinina, N., & Semiletov, I. (2021). Structure and inter-annual variability of the freshened surface layer in the Laptev and East-Siberian Seas during ice-free periods. *Frontiers in Marine Science*, 8, 735011. <https://doi.org/10.3389/fmars.2021.735011>
- Osadchiev, A. A., Frey, D. I., Shchuka, S. A., Tilinina, N. D., Morozov, E. G., & Zavalov, P. O. (2021). Structure of the freshened surface layer in the Kara Sea during ice-free periods. *Journal of Geophysical Research: Oceans*, 126(1), e2020JC016486. <https://doi.org/10.1029/2020JC016486>
- Peterson, B. J., Holmes, R. M., McClelland, J. W., Vörösmarty, C. J., Lammers, R. B., Shiklomanov, A. I., et al. (2002). Increasing river discharge to the Arctic Ocean. *Science*, 298(5601), 2171–2173. <https://doi.org/10.1126/science.1077445>
- Rantanen, M., Karpechko, A. Y., Lippinen, A., Nordling, K., Hyvärinen, O., Ruosteenoja, K., et al. (2022). The Arctic has warmed nearly four times faster than the globe since 1979. *Communications Earth & Environment*, 3(1), 1–10. <https://doi.org/10.1038/s43247-022-00498-3>
- Ray, N. E., Martens, J., Ajmar, M., Tesi, T., Yakushev, E., Gangnus, I., et al. (2024). The role of coastal yedoma deposits and continental shelf sediments in the Arctic Ocean Silicon cycle. *Global Biogeochemical Cycles*, 38(1), e2023GB007746. <https://doi.org/10.1029/2023GB007746>
- Sauerland, L., Ray, N., Martens, J., Tesi, T., Dudarev, O., Gustafsson, Ö., et al. (2024). Sediment properties, carbon dioxide and oxygen fluxes from Siberian Arctic Ocean sediments collected in 2020. (Version 1) [Dataset]. *Bolin Centre Database*. <https://doi.org/10.17043/sauerland-2024-arctic-sediments-1>
- Savelieva, N., Semiletov, I., Vasilevskaya, L., & Pugach, S. (2000). A climate shift in seasonal values of meteorological and hydrological parameters for Northeastern Asia. *0079-6611*, 47(2–4), 279–297. [https://doi.org/10.1016/S0079-6611\(00\)00039-2](https://doi.org/10.1016/S0079-6611(00)00039-2)
- Semiletov, I., Dudarev, O., Luchin, V., Charkin, A., Shin, K., & Tanaka, N. (2005). The East Siberian Sea as a transition zone between Pacific-derived waters and Arctic shelf waters. *Geophysical Research Letters*, 32(10), L10614. <https://doi.org/10.1029/2005GL022490>
- Semiletov, I., Pipko, I., Gustafsson, Ö., Anderson, L. G., Sergienko, V., Pugach, S., et al. (2016). Acidification of East Siberian Arctic Shelf waters through addition of freshwater and terrestrial carbon. *Nature Geoscience*, 9(5), 361–365. <https://doi.org/10.1038/ngeo2695>
- Semiletov, I. P. (1999). Destruction of the coastal permafrost ground as an important factor in biogeochemistry of the Arctic Shelf waters. *Trans. (Doklady) Russian Acad. Sci.*, 368, 679–682.
- Semiletov, I. P., Pipko, I. I., Shakhova, N. E., Dudarev, O. V., Pugach, S. P., Charkin, A. N., et al. (2011). Carbon transport by the Lena River from its headwaters to the Arctic Ocean, with emphasis on fluvial input of terrestrial particulate organic carbon vs. Carbon transport by coastal erosion. *Biogeosciences*, 8(9), 2407–2426. <https://doi.org/10.5194/bg-8-2407-2011>
- Stein, R. & Macdonald, R. W. (Eds.) (2013). *The organic carbon cycle in the Arctic Ocean*. Springer. <https://doi.org/10.1007/978-3-642-18912-8>
- Strauss, J., Laboor, S., Schirrmeister, L., Fedorov, A. N., Fortier, D., Froese, D., et al. (2021). Circum-Arctic map of the Yedoma permafrost domain. *Frontiers in Earth Science*, 9, 758360. <https://doi.org/10.3389/feart.2021.758360>
- Tanski, G., Bröder, L., Wagner, D., Knoblauch, C., Lantuit, H., Beer, C., et al. (2021). Permafrost carbon and CO<sub>2</sub> pathways differ at contrasting coastal erosion sites in the Canadian Arctic. *Frontiers in Earth Science*, 9, 630493. <https://doi.org/10.3389/feart.2021.630493>
- Tesi, T., Semiletov, I., Hugelius, G., Dudarev, O., Kuhry, P., & Gustafsson, Ö. (2014). Composition and fate of terrigenous organic matter along the Arctic land–ocean continuum in East Siberia: Insights from biomarkers and carbon isotopes. *Geochimica et Cosmochimica Acta*, 133, 235–256. <https://doi.org/10.1016/j.gca.2014.02.045>
- Vonk, J. E., & Gustafsson, Ö. (2013). Permafrost-carbon complexities. *Nature Geoscience*, 6(9), 675–676. <https://doi.org/10.1038/ngeo1937>
- Vonk, J. E., Sánchez-García, L., Semiletov, I., Dudarev, O., Eglinton, T., Andersson, A., & Gustafsson, Ö. (2010). Molecular and radiocarbon constraints on sources and degradation of terrestrial organic carbon along the Kolyma paleoriver transect, East Siberian Sea. *Biogeosciences*, 7(10), 3153–3166. <https://doi.org/10.5194/bg-7-3153-2010>
- Vonk, J. E., Sánchez-García, L., van Dongen, B. E., Alling, V., Kosmach, D., Charkin, A., et al. (2012). Activation of old carbon by erosion of coastal and subsea permafrost in Arctic Siberia. *Nature*, 489(7414), 137–140. <https://doi.org/10.1038/nature11392>
- Weiss, R. (1974). Carbon dioxide in water and seawater: The solubility of a non-ideal gas. *Marine Chemistry*, 2(3), 203–215. [https://doi.org/10.1016/0304-4203\(74\)90015-2](https://doi.org/10.1016/0304-4203(74)90015-2)
- Wild, B., Ray, N. E., Lett, C., Davies, A. J., Kirillova, E., Holmstrand, H., et al. (2023). Nitrous oxide dynamics in the Siberian Arctic Ocean and vulnerability to climate change. *Journal of Geophysical Research: Biogeosciences*, 128(5), e2022JG007326. <https://doi.org/10.1029/2022JG007326>
- Wild, B., Shakhova, N., Dudarev, O., Ruban, A., Kosmach, D., Tumskey, V., et al. (2022). Organic matter composition and greenhouse gas production of thawing subsea permafrost in the Laptev Sea. *Nature Communications*, 13(1), 5057. <https://doi.org/10.1038/s41467-022-32696-0>
- Williams, W. J., & Carmack, E. C. (2015). The “interior” shelves of the Arctic Ocean: Physical oceanographic setting, climatology and effects of sea-ice retreat on cross-shelf exchange. *Progress in Oceanography*, 139, 24–41. <https://doi.org/10.1016/j.pocean.2015.07.008>
- Wollenburg, J., & Kuhnt, W. (2000). The response of benthic foraminifers to carbon flux and primary production in the Arctic Ocean. *Marine Micropaleontology*, 40(3), 189–231. [https://doi.org/10.1016/S0377-8398\(00\)00039-6](https://doi.org/10.1016/S0377-8398(00)00039-6)
- You, Q., Cai, Z., Pepin, N., Chen, D., Ahrens, B., Jiang, Z., et al. (2021). Warming amplification over the arctic Pole and third Pole: Trends, mechanisms and consequences. *Earth-Science Reviews*, 217, 103625. <https://doi.org/10.1016/j.earscirev.2021.103625>

## References From the Supporting Information

- Andersson, A., Deng, J., Du, K., Zheng, M., Yan, C., Sköld, M., & Gustafsson, O. (2015). Regionally-varying combustion sources of the January 2013 severe haze events over eastern China. *Environmental Science & Technology*, 49(4), 2038–2043. <https://doi.org/10.1021/es503855e>
- Avnimelech, Y., Ritvo, G., Meijer, L. E., & Kochba, M. (2001). Water content, organic carbon and dry bulk density in flooded sediments. *Aquacultural Engineering*, 25(1), 25–33. [https://doi.org/10.1016/S0144-8609\(01\)00068-1](https://doi.org/10.1016/S0144-8609(01)00068-1)
- Bröder, L., Tesi, T., Andersson, A., Semiletov, I., & Gustafsson, Ö. (2018). Bounding cross-shelf transport time and degradation in Siberian-Arctic land-ocean carbon transfer. *Nature Communications*, 9(1), 806. <https://doi.org/10.1038/s41467-018-03192-1>
- Goñi, M. A., Yunker, M. B., Macdonald, R. W., & Eglinton, T. I. (2000). Distribution and sources of organic biomarkers in arctic sediments from the Mackenzie River and Beaufort Shelf. *Marine Chemistry*, 71(1–2), 23–51. [https://doi.org/10.1016/S0304-4203\(00\)00037-2](https://doi.org/10.1016/S0304-4203(00)00037-2)